available at www.sciencedirect.com
journal homepage: www.europeanurology.com/eufocus

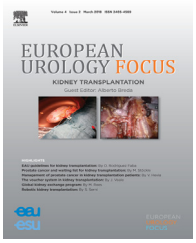

Prostate Cancer

Real-time Augmented Reality Three-dimensional Guided Robotic Radical Prostatectomy: Preliminary Experience and Evaluation of the Impact on Surgical Planning

Riccardo Schiavina [a,b], *Lorenzo Bianchi* [a,b,*], *Simone Lodi* [c], *Laura Cercenelli* [d,e], *Francesco Chessa* [a,b], *Barbara Bortolani* [d], *Caterina Gaudiano* [f], *Carlo Casablanca* [a], *Matteo Droghetti* [a], *Angelo Porreca* [g], *Daniele Romagnoli* [g], *Rita Golfieri* [f], *Francesca Giunchi* [h], *Michelangelo Fiorentino* [h], *Emanuela Marcelli* [c], *Stefano Diciotti* [e], *Eugenio Brunocilla* [a,b]

[a] *Department of Urology, Azienda Ospedaliero-Universitaria di Bologna, Via Albertoni 15, Bologna- Italia;* [b] *Department of Experimental, Diagnostic and Specialty Medicine (DIMES), Cardio-Nephro-Thoracic Sciences Doctorate, University of Bologna, Bologna, Italy;* [c] *Department of Electrical, Electronic and Information Engineering "Guglielmo Marconi", University of Bologna, Bologna, Italy;* [d] *Department of Experimental, Diagnostic and Specialty Medicine (DIMES), Laboratory of Bioengineering, University of Bologna, Bologna, Italy;* [e] *Department of Biomedical and Neuromotor Sciences (DIBINEM), University of Bologna, Bologna, Italy;* [f] *Radiology Unit, Department of Diagnostic Medicine and Prevention, Azienda Ospedaliero-Universitaria di Bologna, Via Albertoni 15, Bologna- Italia;* [g] *Department of Urology, Abano Terme Hospital, Padua, Italy;* [h] *Pathology Department Azienda Ospedaliero-Universitaria di Bologna, Via Albertoni 15, Bologna- Italia*

Article info

Article history:
Accepted August 11, 2020

Associate Editor: Derya Tilki

Keywords:
Augmented reality
Three-dimensional reconstruction
Real-time guided surgery
Robot assisted radical prostatectomy
Index lesion

Abstract

Background: Augmented reality (AR) is a novel technology adopted in prostatic surgery.
Objective: To evaluate the impact of a 3D model with AR (AR-3D model), to guide nerve sparing (NS) during robot-assisted radical prostatectomy (RARP), on surgical planning.
Design, Setting, and Participants: Twenty-six consecutive patients with diagnosis of prostate cancer (PCa) and multiparametric magnetic resonance imaging (mpMRI) results available were scheduled for AR-3D NS RARP.
Intervention: Segmentation of mpMRI and creation of 3D virtual models were achieved. To develop AR guidance, the surgical DaVinci video stream was sent to an AR-dedicated personal computer, and the 3D virtual model was superimposed and manipulated in real time on the robotic console.
Outcome measurements and statistical analysis: The concordance of localisation of the index lesion between the 3D model and the pathological specimen was evaluated using a prostate map of 32 specific areas. A preliminary surgical plan to determinate the extent of the NS approach was recorded based on mpMRI. The final surgical plan was reassessed during surgery by implementation of the AR-3D model guidance.
Results and limitations: The positive surgical margin (PSM) rate was 15.4% in the overall patient population; three patients (11.5%) had PSMs at the level of the index lesion. AR-3D technology changed the NS surgical plan in 38.5% of men on patient-based and in 34.6% of sides on side-based analysis, resulting in overall appropriateness of 94.4%. The 3D model revealed 70%, 100%, and 92% of sensitivity, specificity, and accuracy, respectively, at the 32-area map analysis.
Conclusions: AR-3D guided surgery is useful for improving the real-time identification of the index lesion and allows changing of the NS approach in approximately one out of three cases, with overall appropriateness of 94.4%.

* Corresponding author. Department of Urology, University of Bologna, Azienda Ospedaliero-Universitaria di Bologna, Via Albertoni 15, Bologna- Italia. Tel. +39 0512142334; Fax: +39 0512142750.
E-mail address: lorenzo.bianchi3@gmail.com (L. Bianchi).

https://doi.org/10.1016/j.euf.2020.08.004

Patient summary: Augmented reality three-dimensional guided robot-assisted radical prostatectomy allows identification of the index prostate cancer during surgery, to tailor the surgical dissection to the index lesion and to change the extent of nerve-sparing dissection.

1. Introduction

Major technological innovations applied to robotic surgery have set the "precision medicine" as a novel standard tailored to each patient for the surgical treatment of prostate cancer (PCa) [1]. The ideal nerve-sparing (NS) approach during robot-assisted radical prostatectomy (RARP) should obtain the optimal compromise between the preservation of neurovascular bundles (NVBs) and the higher risk of positive surgical margins (PSMs) [2]. As a consequence, different surgical techniques were introduced to reduce PSMs [3], and several methods have been proposed for "real-time" evaluation of surgical margins [4].

Moreover, multiparametric magnetic resonance imaging (mpMRI) may modify the NVB dissection in one out of three individuals [5–7], with overall appropriateness of 75% [2]. Recently, some authors reported that three-dimensional (3D) models elaborated from two-dimensional (2D) conventional imaging can be used as additional tools to guide surgery [8–12]. Similarly, augmented reality (AR) technology is increasingly adopted in the surgical field [13], and it has also been introduced in prostatic surgery [9,14]. Of note, AR technology could increase the understanding of surgical anatomy and facilitate intraoperative navigation during RARP.

Thus, we aimed to evaluate the impact, on surgical planning, of an AR-3D model to guide surgical dissection during NS RARP for real-time assessment of surgical anatomy and to test the concordance of the reconstructed anatomical 3D models with the final pathological evaluations.

2. Patients and methods

2.1. Study design and participants

We prospectively enrolled 26 consecutive patients with diagnosis of PCa based on positive magnetic resonance imaging (MRI)-targeted fusion biopsy at the index lesion [15], with systematic prostate biopsy and preoperative preserved erectile function (International Index of Erectile Function-5 [IIEF-5] questionnaire score >21 [16]) scheduled for RARP at our institution between April 2019 and September 2019. Participants signed a written informed consent document. The study was conducted after being approved by the Institutional Ethics Committee (IRB approval 4325/2017). The exclusion criteria were contraindications for RARP, undetectable index lesion at preoperative mpMRI, and mpMRI not available. Prior to intervention, patients were addressed to undergo 3D virtual model reconstruction based on preoperative mpMRI findings. Finally, the surgeon performed RARP with the help of the 3D model projected in AR inside the robotic console (AR-3D guided RARP).

2.2. Preoperative imaging

All the mpMRI examinations were performed with a 1.5-T whole-body scanner (Signa HDxt; GE Healthcare, Milwaukee, WI, USA) and a standard eight-channel pelvic phased-array surface coil combined with a disposable endorectal coil (MedRad, Indianola, PA, USA), as described previously [2]. All lesions were scored using the Prostate Imaging Reporting and Data System (PI-RADS)-v2 score [17].

2.3. Three-dimensional model reconstruction

Reconstruction of all 3D virtual models, based on preoperative mpMRI, was carried out by the Laboratory of Bioengineering of the University of Bologna (S. Orsola-Malpighi Hospital), and AR technology was developed by the bioengineers of the Department of Electrical, Electronic and Information Engineering "Guglielmo Marconi", University of Bologna.

Segmentation, that is, labelling of each structure of interest in each mpMRI slice, was achieved using D2P software ("DICOM to PRINT"; 3D Systems Inc., Rock Hill, SC, USA; Fig. 1). Semiautomatic tools (*multislice interpolation* and *threshold segmentation*) of D2P software were adopted to segment the healthy prostatic gland, index lesion, urinary sphincter, and NVBs. D2P was also used to obtain the 3D virtual models that are navigable, by converting the segmented structures to 3D triangulated surface mesh file (STL), using mesh creation methods of D2P (*contour* or *gridbase*; Fig. 2).

To replicate the prostate map used by the pathologist in the whole-mount prostate to localise PCa, the 3D model was stratified in the 3D space, using Meshmixer software (Autodesk Inc., San Rafael, CA, USA), from the base to the apex, from right to left, and from anterior to posterior, leading to 32 specific areas including three to four macrosections in which the seminal vesicles, the base, and the apex were analysed separately (Supplementary Fig. 1).

2.4. AR technology

The AR was delivered through a dedicated hardware and software set-up (Fig. 3). The surgical video stream has been acquired from DaVinci video cart via a frame grabber (USB3HD; Startech, London, Ontario, Canada) and sent to an AR-dedicated PC (equipped with an Intel i7 CPU, 8 GB RAM, and NVIDIA GeForce 840M video card). A 3D view of the virtual model obtained using Meshmixer software (Autodesk Inc.) was superimposed on the operatory field with vMIX (StudioCoast Pty Ltd, Robina, Queensland, Australia). During the intervention, the DaVinci TilePro has been activated in the console and real-time manual alignment has been carried out by a biomedical engineer using a six-degree-of-freedom (3D) mouse (SpaceMouse; 3D Connexion, Munich, Germany). The resulting augmented video stream was also sent to a second external monitor for quality control by the surgeon.

2.5. Surgical technique

All patients underwent RARP using a four-arm DaVinci Xi Surgical System (Intuitive Surgical, Sunnyvale, CA, USA), as described previously [18–20]. The NS approaches were classified according to the patient-

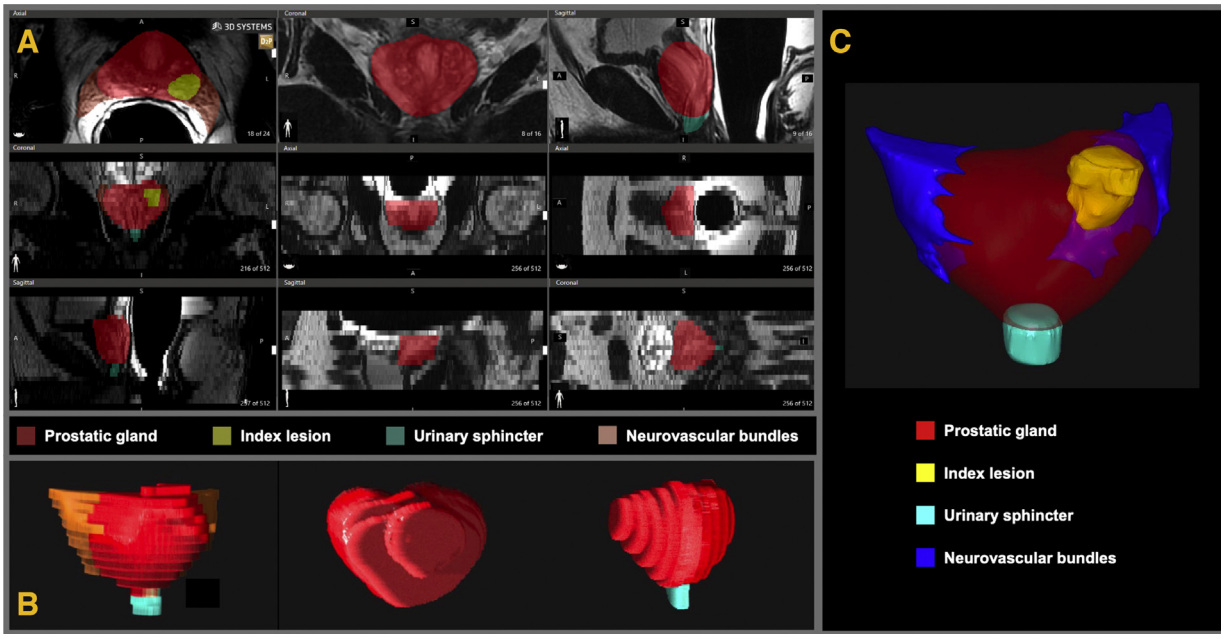

Fig. 1 – Example of process to obtain the 3D virtual anatomical model (A) starting from patient mpMRI, (B) by the segmentation of the anatomical regions of interest (prostatic gland, index lesion, urinary sphincter, and neurovascular bundles) to (C) the final 3D model. 3D = three dimensional; mpMRI = multiparametric magnetic resonance imaging.

based level (considering 26 patients) as bilateral NS, unilateral NS, or non-NS. Indeed, the extent of NVB preservation was recorded on side-based level (considering 52 sides) as grade 1, grade 2, and grade 3–4 according to incremental NS classification, as described by Tewari et al [21]. The main surgeon, when needed, switched to the TilePro visualisation, using AR technology in which the phantom of the 3D model was overlaid to the surgical field (Supplementary Video).

2.6. *Surgical planning*

The surgical plan to evaluate the extent of NS approach was planned by surgeons based on mpMRI findings together with clinical data. Moreover, the effective intraoperative surgical plan regarding the level of NVB preservation [2], both on patient-based and on side-based level, was assessed through a combination of clinical parameters, mpMRI results, and the implemented AR-3D model in the robotic views. At the end of the procedure, the effective intraoperative surgical approach was compared with the preoperative intended planning in order to evaluate the potential success of AR-3D guided technology in the management of surgical dissection.

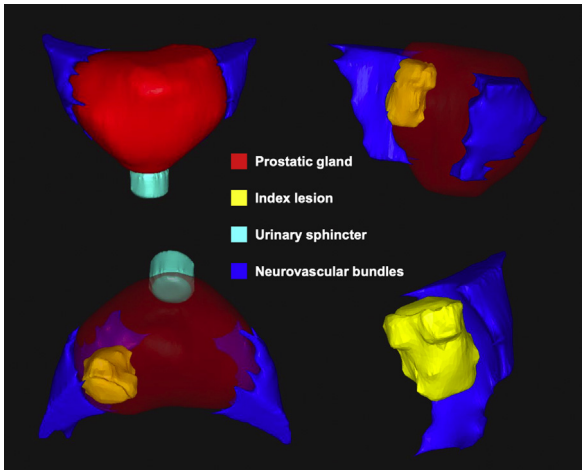

Fig. 2 – Example of the definitive 3D virtual model that can be explored by the surgeon for surgical planning: the model could be rotated and zoomed and is navigable, that is, the surgeon can interact with it changing the transparency of each structure in the 3D rendering, as well as creating a detailed view of the interaction among the different anatomical structures. 3D = three dimensional.

2.7. *Histopathological examination*

Pathological examinations were performed by a single dedicated uropathologist, following a prostate map in which the gland was divided into 32 specific areas (stratified in the 3D space from the base to the apex, from right to left, and from anterior to posterior; Supplementary Fig. 2). The whole-mount histological examinations from the RARP specimens were used as the reference standard, as previously described [22].

2.8. *Statistical analyses*

The McNemar-Bowker test was used to compare the surgical plan regarding NS surgery, before and after its revision following the AR-3D guidance during surgery. The proportion of surgical plan change was recorded on both patient- and side-based level. The appropriateness of surgical plan change was assessed on side-based level and was based on the presence of extracapsular extension (ECE) or PSMs in the NVB area at the final pathological examination [2]: a less oncologically radical approach leading to grade 1 NS was considered appropriate in case of pT2 with negative surgical margins, a less oncologically radical or a more radical approach leading to grade 2 NVB preservation was considered appropriate in case of pT2 or pT3a with negative surgical margins, and a more oncologically radical approach leading to grade 3–4 NVB preservation was considered appropriate in case of pT3a/pT3b regardless surgical margins status. Finally, to evaluate the accuracy of localisation of the index lesion within the 3D model, the presence of suspected index

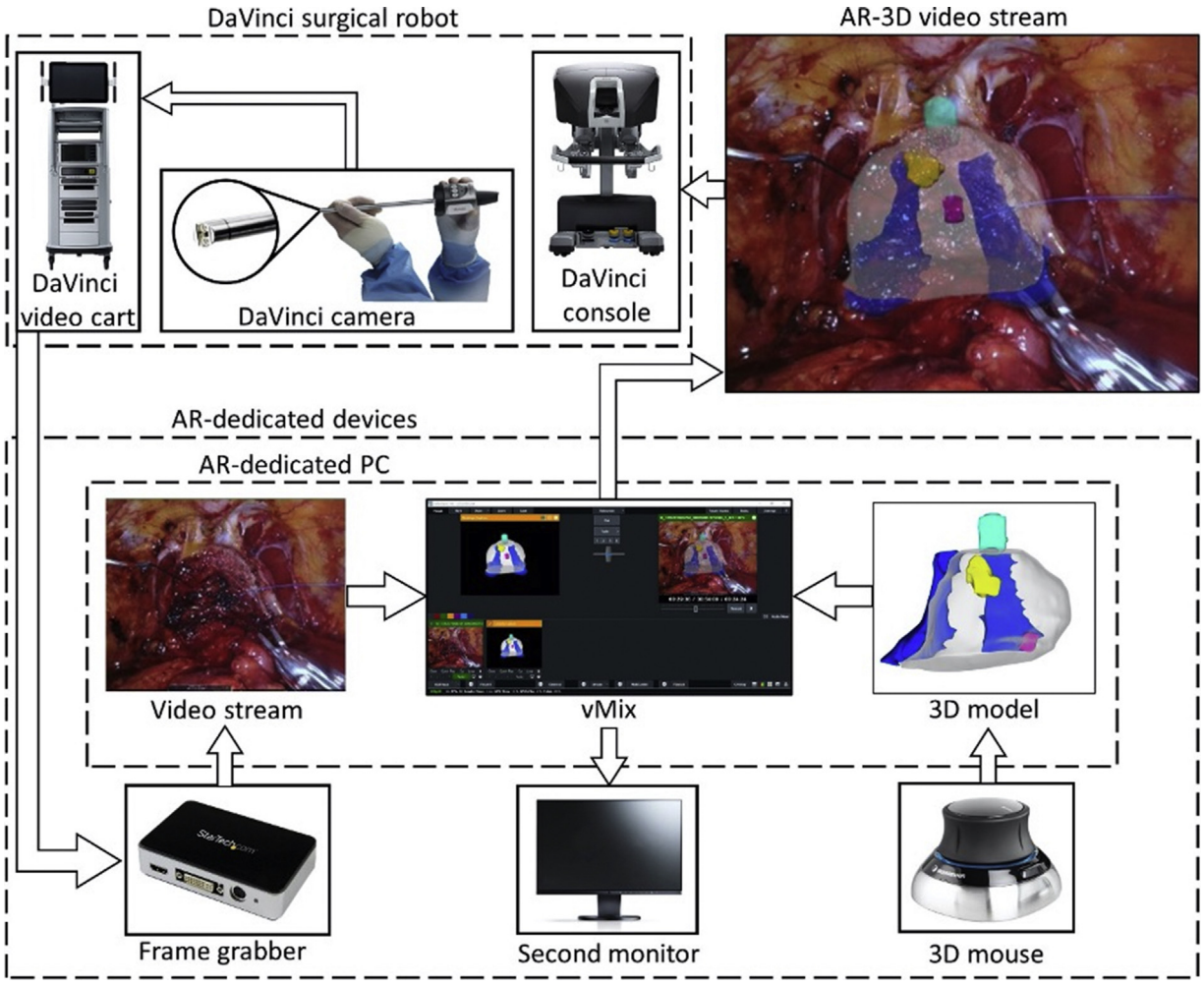

Fig. 3 – A schematic diagram of the hardware and software required to implement the intraoperative use of AR to guide robotic surgery. AR = augmented reality; 3D = three dimensional.

PCa in each of the 32 prostatic areas obtained from model stratification was assessed by visual inspection, and it was compared with the presence of PCa in the corresponding 32 prostatic areas evaluated separately at pathological examination, following the prostate map analysis (Supplementary Fig. 3). A p value of <0.05 was considered statistically significant. All statistical tests were performed using SPSS 22.0.

3. Results

Demographic and clinical characteristics are summarised in Table 1. Preoperative mpMRI reported organ-confined index lesion in 23 patients and suspected ECE in three individuals; index lesions were classified as PI-RADS 3, 4, and 5 in nine (34.6%), nine (34.6%), and eight (30.8%) men, respectively. Overall, the PSM rate was 15.4%: one (5.3%) PSM in pT2, two (33.3%) PSMs in pT3a, and one (100%) PSM in pT3b. Only three patients (11.5%) had PSMs at the level of the index lesion detected with the 3D-AR model (Table 2). Overall, twos men experienced postoperative complication (Clavien <3). The continence recovery rates (zero or one safety pad) were 57.7%, 73.1%, 88.5%, and 92.3% at catheter removal, 1 mo, 3 mo, and 6 mo, respectively. The erectile function recovery rate (IIEF-5 >21 with or without phosphodiesterase 5 inhibitor) was 23.1% at 1 mo, 53.8% at 3 mo, and 65% at 6 mo. No patient had biochemical recurrence at a median follow-up of 8 mo (Supplementary Table 1). On side-based level, grade 1, 2, and 3–4 NS would have been performed, respectively, in 23 (44.2%), six (11.5%), and 23 (44.2%) sides without the 3D-AR model; however, grade 1, 2, and 3–4 NS was finally performed, respectively, in 19 (36.5%), 17 (32.7%), and 16 (30.8%) sides with the use of 3D-AR technology ($p = 0.02$; Supplementary Table 2). The initial surgical plan of NS techniques was changed by the use of an AR-3D model in 38.5% of men. In three (30%) cases, surgery was changed to more radical approaches, while in seven (70%) cases, the NS approach was attempted (less radical approach; Table 3).

The use of AR-3D technology induced the surgeon to change the NS surgical plan in 18 (34.6%) sides with overall appropriateness of 94.4% (Table 4). In 50% of cases, surgery was changed towards a more radical approach (appropriateness of 77.8%); in the other half of cases, the surgical plan was changed into a less radical approach (appropriateness of 88.9%). Finally, Supplementary Figure 3 depicts the concordance between the 3D model and the whole-mount

Table 1 – Overall patient characteristics and mpMRI data (*n* = 26)

Variable	Overall
Age (yr), median (IQR)	63 (56–70)
BMI, median (IQR)	27 (26–29.3)
CCI, median (IQR)	1 (0–1)
PSA (ng/ml), median (IQR)	6.7 (5.5–8)
IIEF-5, median (IQR)	23 (21–24)
Number of positive biopsy cores, median (IQR)	4 (2–6)
Positive DRE, *n* (%)	12 (46.2)
Biopsy Gleason grade group, *n* (%)	
1	4 (15.4)
2	11 (42.3)
3	5 (19.2)
4	6 (23.1)
5	0 (0)
D'Amico risk group, *n* (%)	
Low	4 (15.4)
Intermediate	11 (42.3)
High	11 (42.3)
mpMRI results, *n* (%)	
Negative	0 (0)
Organ-confined lesion	23 (88.5)
ECE	3 (11.5)
SVI	0 (0)
PI-RADS-v2, *n* (%)	
3	9 (34.6)
4	9 (34.6)
5	8 (30.8)
Index lesion's volume (mm), median (IQR)	16.5 (10–20)
Side of the index lesion, *n* (%)	
Right lobe	12 (46.2)
Left lobe	14 (53.8)
Bilateral	0 (0)
Site of the index lesion, *n* (%)	
Apex	11 (42.3)
Mid gland	8 (30.8)
Base	7 (26.9)
Location of the index lesion, *n* (%)	
Posterior	21 (80.8)
Posterior medial	6 (23.1)
Posterior lateral	15 (57.7)
Anterior	5 (19.2)
Anterior lateral	3 (11.5)
Transition zone	2 (7.7)

BMI = body mass index; CCI = Charlson Comorbidity Index; DRE = digital rectal examination; ECE = exacapsular extension; IIEF-5 = International Index of Erectile Function-5; IQR = interquartile range; mpMRI = multiparametric magnetic resonance imaging; PI-RADS-v2 = Prostate Imaging Reporting and Data System version 2; PSA = prostate-specific antigen; SVI = seminal vesicle invasion.

Table 2 – Pathological characteristics in overall patient population (*n* = 26)

Variable	Overall
Pathologic Gleason grade group, *n* (%)	
1	0 (0)
2	14 (53.8)
3	6 (23.1)
4	3 (11.5)
5	3 (11.5)
Pathological stage, *n* (%)	
pT2	19 (73.1)
pT3a	6 (23.1)
pT3b	1 (3.8)
Tumour volume (ml), median (IQR)	10 (6.5–16.3)
PSMs, *n* (%)	4 (15.4)
PSMs according to pathological stage, *n* (%)	
pT2	1 (5.3)
pT3a	2 (33.3)
pT3b	1 (100)
Site of PSMs, *n* (%)	
Apex	3 (11.5)
Posterolateral	1 (3.8)
Posterolateral PSMs according to nerve-sparing approach by Tewari et al [21] (side based), *n* (%)	
Grade 1	0 (0)
Grade 2	1 (5.9)
Grade 3–4	1 (6.3)
PSMs at index lesion level, *n* (%)	
Negative	23 (88.5)
Positive	3 (11.5)

IQR = interquartile range; PSM = positive surgical margin.

Table 3 – Nerve-sparing surgical plan change on a patient-based analysis with the use of 3D-AR technology (*n* = 26)

Without surgical plan change, *n* (%)	16 (61.5)
With surgical plan change, *n* (%)	10 (38.5)
More radical approach, *n* (%)	
Bilateral NS → no NS	3 (30)
Bilateral NS → unilateral NS	1 (33.3)
Unilateral NS → no NS	2 (66.7)
	0 (0)
Less radical approach, *n* (%)	
No NS → unilateral NS	7 (70)
No NS → bilateral NS	2 (28.6)
Unilateral NS → bilateral NS	4 (57.1)
	1 (14.3)

3D-AR = three-dimensional augmented reality; NS = nerve sparing.

specimen according to the 32 prostatic areas to localise the index lesion: the 3D model revealed 70%, 100%, and 92% of sensitivity, specificity, and accuracy, respectively, in the prostate map analysis (Supplementary Table 3).

4. Discussion

In the era of precision medicine, the evolution of real-time imaging-guided technology is an increasing need to improve the surgical dissection for a tailored surgery of PCa [14]. Of note, continuous efforts and technique modifications aiming to reduce PSMs and to preserve both the periprostatic NVBs [21,23] and the periapical tissue [3] are proposed to obtain better surgical outcomes [24–26]. Despite the use of mpMRI representing a routine practice to guide NS surgery nowadays [2], it is not a "real-time" method to evaluate the surgical anatomy during RARP. Thus, "in vivo" assessment of prostatic gland and periprostatic tissue has gained special interest in PCa surgery [4]. High-fidelity 3D models represent one of the most appealing methods for better understanding of surgical anatomy and guiding surgical planning in different fields [10,11,14,27]. As a consequence, the use of 3D models in urology showed a significant impact on surgical planning and decision-making process that may influence patients' outcomes [28]. Porpiglia and coworkers [14,29] have reported their preliminary experience with the use of AR technology. Thus, the AR-3D guided surgery is proposed to facilitate the intraoperative "real-time" navigation and dissection in crucial steps.

Table 4 – Nerve-sparing surgical plan change and relative appropriateness on side-based analysis with the use of 3D-AR technology (*n* = 52)

	Number	Appropriateness
Without intraoperative nerve sparing plan change, *n* (%)	34 (65.4)	24/34 (70.6)
With intraoperative nerve sparing plan change, *n* (%)	18 (34.6)	17/18 (94.4)
More radical approach, *n* (%)		
Grade[a] 1 → grade 2	9 (50)	7/9 (77.8)
Grade 1 → grade 3–4	4 (44.4)	4/4 (100)
Grade 2 → grade 3–4	5 (55.6)	3/5 (60)
	0 (0)	0 (0)
Less radical approach, *n* (%)		
Grade 2 → grade 1	9 (50)	8/9 (88.9)
Grade 3–4 → grade 2	1 (11.1)	1/1 (100)
Grade 3–4 → grade 1	6 (66.7)	5/6 (83.3)
	2 (22.2)	2/2 (100)

3D-AR = three-dimensional augmented reality.
[a] Grade of nerve sparing according to the classification proposed by Tewari et al [21].

Several findings are noteworthy in our study. First, the 3D virtual model overlapped the DaVinci console through TilePro connection proved to be feasible to define the anatomy of the prostatic glands and the index lesion, as demonstrated by the good concordance with the whole-mount pathological analysis. Previously, Porpiglia et al [14,30] showed that AR-3D models were able to identify the index lesion in 100% of patients, with a mismatch between the 3D reconstruction and the scanned prostate recorded from 1 to 5 mm [14]. In our cohort, we used a simple method (a prostate map stratified into 32 specific areas) to validate the 3D model in terms of the localisation of the index lesion, considering the whole-mount pathological specimens as reference: overall, the 3D model revealed 92% accuracy to localise the index lesion. The proposed prostate map analysis has two main advantages: firstly, the 32-area prostate map on the 3D model is easy to obtain using the free software Meshmixer; secondly, the proposed prostate map analysis to compare the 32 areas on the 3D model and the pathological specimen is able to assess the concordance/nonconcordance to localise the index lesion in the same areas or the presence of PCa in areas nearby the index lesion.

Second, for the first time ever, we evaluated the impact of AR-3D guided surgery to modify the real-time intraoperative approach to NS on both patient- and side-based analyses. The surgical plan was changed through real-time AR-3D visualisation, in 38.5% patients and in 34.6% sides with safe results in terms of PSMs (15.4% overall). Third, the change in the NS plan due to AR-3D was appropriate in the vast majority of cases: overall, in 50% of sides, AR-3D led to more radical NS (appropriateness of 77.8%), while in the remaining half of the cases, it led to less radical NS (appropriateness of 88.9%). Fourth, the AR-3D guided approach to NVBs allows modulation of the NS approach tailored to the index lesion, by resecting more tissue nearby the lesion and preserving more tissue outside the lesion, aiming to maximise both oncological and functional outcomes. Thus, PSMs at the level of index lesion were 11.5%, and the erectile function recovery was 65% at 6 mo in patients referred to NS RARP. These findings suggest that the accuracy offered by AR-3D technology could allow for a "real-time" robotic procedure tailored to the patient-specific anatomy and the specific cancer location. Future applications of intraoperative frozen section targeted to the index lesion and guided by AR-3D models could allow further improvement of surgical outcomes.

Despite several strengths, our study is not devoid of limitations. First, in spite of the prospective nature of the study, the number of patients included is limited. Second, we used rigid 3D prostate models that do not represent the tissue deformation during surgical dissection and the biological realism necessary to create more functional and dynamic overlapping. Third, the lack of a control group of patients submitted to RARP without the use of an AR-3D model did not allow for the assessment of the real impact of this technology to modify the surgical approach. Furthermore, the adoption of different definitions of appropriateness of a surgical plan would affect the final results. Moreover, the superimposed screen with the 3D model can create some problems during the dissection, since the surgeons need to switch from the conventional to the TilePro view that consists of a double and smaller screen. Fourth, we also included the first patients treated with this novel technology, with a possible effect being prolonging the surgical time due to the learning curve process. Indeed, we found that two to five cases are needed for both the surgeon and the bioengineer to improve the overlap of the 3D model in the surgical field. Finally, the major limitations of AR-assisted surgery consist of possible registration inaccuracy, translating into a poor navigation precision, and the need for manual external adjustments of the 3D model overlapping on the surgical field [9]. Thus, automatic registration of the 3D model to the surgical view, based on artificial intelligence, could be a further implementation to obtain automated overlapping of the 3D virtual model inside the DaVinci console liable for the organ movement during surgery.

5. Conclusions

The use of AR-3D guided surgery can be a feasible tool to improve the real-time identification of the index lesion, and it could be useful for modulating the NS approach during

RARP. The surgical plan change after the intraoperative adoption of AR-3D guidance technology was recorded in approximately one out of three cases, with overall appropriateness of 94.4%.

Author contributions: Lorenzo Bianchi had full access to all the data in the study and takes responsibility for the integrity of the data and the accuracy of the data analysis.*Study concept and design*: L. Bianchi, Chessa, Schiavina.

Acquisition of data: Lodi, Cercenelli, Bortolani, Diciotti, Romagnoli.

Analysis and interpretation of data: L. Bianchi, Gaudiano, Droghetti, Casablanca, Cercenelli.

Drafting of the manuscript: L. Bianchi, Marcelli, Gaudiano, Schiavina, Cercenelli, Golfieri.

Critical revision of the manuscript for important intellectual content: Schiavina, Golfieri, Diciotti, Marcelli, Gaudiano, Porreca.

Statistical analysis: L. Bianchi, Droghetti, Chessa.

Obtaining funding: Porreca, Diciotti, Marcelli.

Administrative, technical, or material support: Marcelli, Gaudiano, Diciotti, Schiavina, Golfieri.

Supervision: Schiavina, Diciotti, Porreca, Marcelli.

Other: None.***Financial disclosures:*** Lorenzo Bianchi certifies that all conflicts of interest, including specific financial interests and relationships and affiliations relevant to the subject matter or materials discussed in the manuscript (eg, employment/affiliation, grants or funding, consultancies, honoraria, stock ownership or options, expert testimony, royalties, or patents filed, received, or pending), are the following: None.

***Funding/Support and role of the sponsor*:** The project was supported by a Technology Research Grant by Intuitive Surgical for the development of AR technology in robotic surgery.

Appendix A. Supplementary data

Supplementary material related to this article can be found, in the online version, at https://doi.org/10.1016/j.euf.2020.08.004.

References

[1] Checcucci E, Amparore D, Fiori C, et al. 3D imaging applications for robotic urologic surgery: an ESUT YAUWP review. World J Urol 2020;38:869–81.

[2] Schiavina R, Bianchi L, Borghesi M, et al. MRI displays the prostatic cancer anatomy and improves the bundles management before robot-assisted radical prostatectomy. J Endourol 2018;32:315–21.

[3] Bianchi L, Turri FM, Larcher A, et al. A novel approach for apical dissection during robot-assisted radical prostatectomy: the "collar" technique. Eur Urol Focus 2018;4:677–85.

[4] Eissa A, Zoeir A, Sighinolfi MC, et al. Real-time" assessment of surgical margins during radical prostatectomy: state-of-the-art. Clin Genitourin Cancer 2020;18:95–104.

[5] McClure TD, Margolis DJA, Reiter RE, et al. Use of MR imaging to determine preservation of the neurovascular bundles at robotic-assisted laparoscopic prostatectomy. Radiology 2012;262:874–83.

[6] Park BH, Jeon HG, Jeong BC, et al. Influence of magnetic resonance imaging in the decision to preserve or resect neurovascular bundles at robotic assisted laparoscopic radical prostatectomy. J Urol 2014;192:82–8.

[7] Kozikowski M, Malewski W, Michalak W, Dobruch J. Clinical utility of MRI in the decision-making process before radical prostatectomy: systematic review and meta-analysis. PLoS One 2019;14:e0210194.

[8] Porpiglia F, Fiori C, Checcucci E, Amparore D, Bertolo R. Hyperaccuracy three-dimensional reconstruction is able to maximize the efficacy of selective clamping during robot-assisted partial nephrectomy for complex renal masses. Eur Urol 2018;74:651–60.

[9] Bertolo R., Hung A, Porpiglia F, Bove P, Schleicher M, Dasgupta P. Systematic review of augmented reality in urological interventions: the evidences of an impact on surgical outcomes are yet to come. World J Urol. In press. DOI: 10.1007/s00345-019-02711-z

[10] Schiavina R, Bianchi L, Borghesi M, et al. Three-dimensional digital reconstruction of renal model to guide preoperative planning of robot-assisted partial nephrectomy. Int J Urol 2019;26:931–2.

[11] Bianchi L, Schiavina R, Barbaresi U, et al. 3D reconstruction and physical renal model to improve percutaneous puncture during PNL. Int Braz J Urol 2019;45:1281–2.

[12] Borghesi M, Schiavina R, Gan M, Novara G, Mottrie A, Ficarra V. Expanding utilization of robotic partial nephrectomy for clinical T1b and complex T1a renal masses. World J Urol 2013;31:499–504.

[13] Badiali G, Cercenelli L, Battaglia S, et al. Review on augmented reality in oral and cranio-maxillofacial surgery: toward "surgery-specific" head-up displays. IEEE Access 2020;8:59015–28.

[14] Porpiglia F, Fiori C, Checcucci C, Amparore S, Bertolo R. Augmented reality robot-assisted radical prostatectomy: preliminary experience. Urology 2018;115:184.

[15] Ahmed HU. The index lesion and the origin of prostate cancer. N Engl J Med 2009;361:1704–6.

[16] Cappelleri JC, Rosen RC, Smith MD, Mishra A, Osterloh IH. Diagnostic evaluation of the erectile function domain of the International Index of Erectile Function. Urology 1999;54:346–51.

[17] Weinreb JC, Barentsz JO, Choyke PL, et al. PI-RADS Prostate Imaging - Reporting and Data System: 2015, version 2. Eur Urol 2016;69:16–40.

[18] Mottrie A, De Naeyer G, Schatteman P, Frumenzio E, Rossanese M, Ficarra V. Robot-assisted radical prostatectomy: tips, tricks and pitfalls. Minerva Urol Nefrol 2012;64:89–96.

[19] Porreca A, D'agostino D, Dandrea M, et al. Bidirectional barbed suture for posterior musculofascial reconstruction and knotless vesicourethral anastomosis during robot-assisted radical prostatectomy. Minerva Urol Nefrol 2018;70:319–25.

[20] Porreca A, Salvaggio A, Dandrea M, et al. Robotic-assisted radical prostatectomy with the use of barbed sutures. Surg Technol Int 2017;30:39–43.

[21] Tewari AK, Ali A, Metgud S, et al. Functional outcomes following robotic prostatectomy using athermal, traction free risk-stratified grades of nerve sparing. World J Urol 2013;31:471–80.

[22] Bianchi L, Schiavina R, Borghesi M, et al. Patterns of positive surgical margins after open radical prostatectomy and their association with clinical recurrence. Minerva Urol Nefrol 2020;72:464–73.

[23] Patel VR, Schatloff O, Chauhan S, et al. The role of the prostatic vasculature as a landmark for nerve sparing during robot-assisted radical prostatectomy. Eur Urol 2012;61:571–6.

[24] Schiavina R, Borghesi M, Dababneh H, et al. Survival, continence and potency (SCP) recovery after radical retropubic prostatectomy: a long-term combined evaluation of surgical outcomes. Eur J Surg Oncol 2014;40:1716–23.

[25] Schiavina R, Bertaccini A, Franceschelli A, et al. The impact of the extent of lymph-node dissection on biochemical relapse after radical prostatectomy in node-negative patients. Anticancer Res 2010;30:2297–302.

[26] Farolfi A, Ceci F, Castellucci P, et al. (68)Ga-PSMA-11 PET/CT in prostate cancer patients with biochemical recurrence after radical prostatectomy and PSA <0.5 ng/ml. Efficacy and impact on treatment strategy. Eur J Nucl Med Mol Imaging 2019;46:11–9.

[27] Shirk JD, Thiel DD, Wallen EM, et al. Effect of 3-dimensional virtual reality models for surgical planning of robotic-assisted partial

nephrectomy on surgical outcomes: a randomized clinical trial. JAMA Netw Open 2019;2:e1911598.

[28] Cacciamani GE, Okhunov Z, Meneses AD, et al. Impact of three-dimensional printing in urology: state of the art and future perspectives. A systematic review by ESUT-YAUWP Group. Eur Urol 2019;76:209–21.

[29] Porpiglia F, Bertolo R, Amparore D, et al. Augmented reality during robot-assisted radical prostatectomy: expert robotic surgeons' on-the-spot insights after live surgery. Minerva Urol Nefrol 2018;70:226–9.

[30] Porpiglia F, Checcucci E, Amparore D, et al. Three-dimensional elastic augmented-reality robot-assisted radical prostatectomy using hyperaccuracy three-dimensional reconstruction technology: a step further in the identification of capsular involvement. Eur Urol 2019;76:505–14.